

August 2003

Implications of the DAMA and CRESST experiments for mirror matter-type dark matter

R. Foot¹

*School of Physics,
University of Melbourne,
Victoria 3010 Australia*

Mirror atoms are expected to be a significant component of the galactic dark matter halo if mirror matter is identified with the non-baryonic dark matter in the Universe. Mirror matter can interact with ordinary matter via gravity and via the photon-mirror photon kinetic mixing interaction – causing mirror charged particles to couple to ordinary photons with effective electric charge ϵe . This means that the nuclei of mirror atoms can elastically scatter off the nuclei of ordinary atoms, leading to nuclear recoils, which can be detected in existing dark matter experiments. We show that the dark matter experiments most sensitive to this type of dark matter candidate (via the nuclear recoil signature) are the DAMA/NaI and CRESST/Sapphire experiments. Furthermore, we show that the impressive annual modulation signal obtained by the DAMA/NaI experiment can be explained by mirror matter-type dark matter for $|\epsilon| \sim 4 \times 10^{-9}$ and is supported by the CRESST/Sapphire data. This value of $|\epsilon|$ is consistent with the value obtained from various solar system anomalies including the Pioneer spacecraft anomaly, anomalous meteorite events and lack of small craters on the asteroid Eros. It is also consistent with standard BBN.

¹E-mail address: rfoot@unimelb.edu.au

The DAMA/NaI experiment[1, 2] has been searching for dark matter and has obtained some very exciting positive results which merit serious consideration. While they have interpreted their data in terms of weakly interacting heavy particles an alternative interpretation will be suggested here.

In the DAMA/NaI experiment the target consists of 100 kg of radiopure NaI. The aim of the experiment is to measure recoil energy of the Na, I atoms due to interactions of dark matter particles with their detector. Due to the Earth's motion around the sun, the rate should experience a small annual modulation:

$$A \cos 2\pi(t - t_0)/T \quad (1)$$

According to the DAMA analysis[2], they indeed find such a modulation over 7 annual cycles at more than 6σ C.L. Their data fit gives $T = (1.00 \pm 0.01)$ year and $t_0 = 144 \pm 22$, consistent with the expected values. [The expected value for t_0 is 152 (2 June), where the Earth's velocity, v_E , reaches a maximum with respect to the galaxy]. The strength of their signal is $A = (0.020 \pm 0.003)$ cpd/kg/keV.

The DAMA collaboration have interpreted these impressive results as evidence for heavy weakly interacting dark matter particles. However, another possibility is that this experiment has observed the impacts of galactic mirror atoms, as will shortly be explained.

Mirror matter is predicted to exist if nature exhibits an exact unbroken mirror symmetry (for reviews and more complete set of references, see Ref.[3]). For each type of ordinary particle (electron, quark, photon etc) there is a mirror partner (mirror electron, mirror quark, mirror photon etc), of the same mass. The two sets of particles form parallel sectors each with gauge symmetry G (where $G = SU(3) \otimes SU(2) \otimes U(1)$ in the simplest case) so that the full gauge group is $G \otimes G$. The unbroken mirror symmetry maps $x \rightarrow -x$ as well as ordinary particles into mirror particles. Exact unbroken time reversal symmetry also exists, with standard CPT identified as the product of exact T and exact P[4].

Ordinary and mirror particles can interact with each other by gravity and via the photon-mirror photon kinetic mixing interaction:

$$\mathcal{L} = \frac{\epsilon}{2} F^{\mu\nu} F'_{\mu\nu} \quad (2)$$

where $F^{\mu\nu}$ ($F'_{\mu\nu}$) is the field strength tensor for electromagnetism (mirror electromagnetism)². Photon-mirror photon mixing causes mirror charged particles to couple to ordinary photons with a small effective electric charge, ϵe [4, 7, 8]. Interestingly, the existence of photon-mirror photon kinetic mixing allows mirror matter to explain a number of puzzling observations, including the Pioneer spacecraft anomaly[9, 10], anomalous

²Given the constraints of gauge invariance, renormalizability and mirror symmetry it turns out[4] that the only allowed non-gravitational interactions connecting the ordinary particles with the mirror particles are via photon-mirror photon kinetic mixing and via a Higgs-mirror Higgs quartic interaction, $\mathcal{L} = \lambda \phi^\dagger \phi \phi'^\dagger \phi'$. If neutrinos have mass, then ordinary - mirror neutrino oscillations may also occur[5, 6].

meteorite events[11, 12] and the unexpectedly low number of small craters on the asteroid 433 Eros[13, 14]. It turns out that these explanations and other constraints[15, 16] suggest that ϵ is in the range

$$10^{-9} \lesssim |\epsilon| \lesssim 10^{-6}. \quad (3)$$

More generally, mirror matter is a rather obvious candidate for the non-baryonic dark matter in the Universe because:

- It is well motivated from fundamental physics since it is required to exist if parity and time reversal symmetries are exact, unbroken symmetries of nature.
- It is necessarily dark and stable. Mirror baryons have the same lifetime as ordinary baryons and couple to mirror photons instead of ordinary photons.
- Mirror matter can provide a suitable framework for which to understand the large scale structure of the Universe[17].
- Recent observations from WMAP[18] and other experiments suggest that the cosmic abundance of non-baryonic dark matter is of the same order of magnitude as ordinary matter $\Omega_b \sim \Omega_{dark}$. A result which can naturally occur if dark matter is identified with mirror matter[19].

If mirror matter is identified as the non-baryonic dark matter, then the dark matter halo will consist of compact objects such as mirror stars and planets, as well as a mirror gas and dust component. Evidence for mirror stars arises from MACHO observations [20, 21] (and to some extent from the puzzling ‘isolated’ planets[22]) while the existence of close-in extrasolar planets can also be viewed as mirror matter manifestations[23]. The amount of material in compact form is probably less than 50% (coming from the MACHO upper limit). Thus we expect a dark matter halo with a significant gas/dust component containing mirror H' , He' + heavier mirror elements. Assuming a local halo dark matter energy density of 0.3 GeV/cm^3 , then the number densities of $A' = H', He'$ and heavier elements is then given by

$$n_{A'} = \xi_{A'} \frac{0.3 \text{ GeV}}{M_{A'}} \text{ cm}^{-3} \quad (4)$$

where $\xi_{A'} \equiv \rho_{A'}/(0.3 \text{ GeV/cm}^3)$ is the A' proportion (by mass) of the halo dark matter. As discussed above, a plausible value for $\sum_{A'} \xi_{A'}$ is $\sim 1/2$.

Arguments from early Universe cosmology (mirror BBN)[17] suggest that He' dominates over H' , quite unlike the case with ordinary matter. Mirror elements heavier than H', He' will presumably come from nucleosynthesis within mirror stars, qualitatively similar to the ordinary matter case. In the ordinary matter case, the galactic relative (mass) abundance of elements heavier than H, He (collectively called ‘metals’ in the astrophysics literature) is estimated[24] to be roughly $Z_g \sim 0.02 \Rightarrow \xi_{Metals}/\xi_{He} \sim 0.10$. These heavier elements are made up primarily ($> 90\%$) of O, Ne, N, C which have $M_A/M_P \simeq 16 \pm 4$, $Z = 8 \pm 2$. Thus, oxygen provides an excellent ‘average’ for ordinary elements heavier than helium – except perhaps for iron [which is about 10 times

less abundant (by mass) than oxygen]. In the case of mirror element abundances, we would expect a *qualitatively* similar picture, i.e. O' (and elements with nearby atomic number) should dominate the energy density after H' , He' , with a possible small Fe' contribution. Thus we need only consider four mirror elements: H' , He' , O' , Fe' (where O' stands for Oxygen and nearby elements). Of course, *quantitatively*, the ratios $\xi_{O'}/\xi_{He'}$, $\xi_{Fe'}/\xi_{O'}$ are quite uncertain because of the different initial values for He'/H' (coming from mirror BBN) and other different initial conditions. Although the proportion of the various mirror elements in the halo (gas/dust ratio etc) is uncertain, the mass scale is not a free parameter: mirror hydrogen, H' , is predicted to have exactly the same mass as ordinary hydrogen, i.e. $M_{H'} = 0.94 \text{ GeV}$, mirror helium, He' , has mass $M_{He'} = 3.76 \text{ GeV}$ etc.

In an experiment such as DAMA/NaI, the measured quantity is the recoil energy, E_R , of a target atom. The minimum velocity of a mirror atom of mass $M_{A'}$ impacting on a target atom of mass M_A is related to E_R via the kinematic relation:

$$v_{min} = \sqrt{\frac{(M_A + M_{A'})^2 E_R}{2M_A M_{A'}}}. \quad (5)$$

Interestingly, most of the existing dark matter experiments are not very sensitive to mirror matter-type dark matter because v_{min} [Eq.(5)] turns out to be too high. This is because they either use target elements which are too heavy (i.e. large M_A) or have a E_R threshold which is too high. For example, the CDMS experiment uses Ge as the target material and has a threshold of 10 keV[25]. This means that $v_{min} \approx 1600 \text{ km/s}$ (for He'). Although there would be no cutoff velocity at the galactic escape velocity for He' due to He' self interactions the number of He' with such high velocities would be negligible. The existing experiments with the greatest sensitivity to light mirror elements are the DAMA/NaI[1, 2] and the CRESST/sapphire experiments[26]. Both of these experiments will be examined in detail.

When mirror matter encounters ordinary matter, the nuclei of the ordinary atoms (of mass M_A , atomic number Z) and mirror atoms (of mass $M_{A'}$, atomic number Z') can (Rutherford) scatter off each other, with center of mass cross section: ³

$$\left(\frac{d\sigma}{d\Omega}\right)_{\text{elastic}} = \frac{e^2 \alpha^2 Z^2 Z'^2 M_{red}^2}{4M_{A'}^4 v_{cm}^4 \sin^4 \frac{\theta_s}{2}} \quad (6)$$

where v_{cm} is the center of mass velocity of the impacting mirror atom and $M_{red} = M_A M_{A'}/(M_A + M_{A'})$ is the reduced mass. Due to the screening effects of the atomic electrons, the cross section is modified (and becomes suppressed) at small scattering angles [$\theta_s \lesssim 1/(M_{A'} v r_0)$ with $r_0 \sim 10^{-9} \text{ cm}$]. This cross section can be expressed in terms of the recoil energy of the ordinary atom, E_R and lab velocity, v (i.e. the velocity in Earth rest frame)

$$\frac{d\sigma}{dE_R} = \frac{\lambda}{E_R^2 v^2} \quad (7)$$

³The finite size of the nucleus can be taken into account with a form factor in the usual way. Note also that unless otherwise stated, we use natural units where $\hbar = c = 1$.

where

$$\lambda \equiv \frac{2\pi\epsilon^2\alpha^2Z^2Z'^2}{M_A}. \quad (8)$$

The interaction rate is then given by,

$$\begin{aligned} \frac{dR}{dE_R} &= \sum_{A'} N_T n_{A'} \int \frac{d\sigma}{dE_R} \frac{f(v, v_E)}{k} |v| d^3v \\ &= \sum_{A'} N_T n_{A'} \frac{\lambda}{E_R^2} \int_{v_{min}(E_R)}^{\infty} \frac{f(v, v_E)}{k|v|} d^3v \end{aligned} \quad (9)$$

where N_T is the number of target atoms per kg of detector⁴ and $f(v, v_E)/k$ is the velocity distribution of the mirror element, A' , with v being the velocity relative to the Earth, and v_E is the Earth velocity relative to the dark matter distribution. The lower velocity limit, $v_{min}(E_R)$, is obtained from Eq.(5), while the upper limit, $v_{max} = \infty$, because of A' self interactions (as we will explain in a moment).

The velocity integral in Eq.(9),

$$I(E_R) \equiv \int_{v_{min}(E_R)}^{\infty} \frac{f(v, v_E)}{k|v|} d^3v \quad (10)$$

is standard (as it occurs also in the usual WIMP interpretation) and can easily be evaluated in terms of error functions assuming a Maxwellian dark matter distribution[27], $f(v, v_E)/k = (\pi v_0^2)^{-3/2} \exp[-(v + v_E)^2/v_0^2]$,

$$I(E_R) = \frac{1}{2v_0 y} [erf(x + y) - erf(x - y)] \quad (11)$$

where

$$x \equiv \frac{v_{min}(E_R)}{v_0}, \quad y \equiv \frac{v_E}{v_0}. \quad (12)$$

For standard non-interacting WIMPs, v_0 is expected to be in the (90% C.L.) range[28],

$$170 \text{ km/s} \lesssim v_0 \lesssim 270 \text{ km/s}. \quad (13)$$

In the case of a halo composed of H' , He' , heavier mirror elements and dust particles, there are important differences due to mirror particle self interactions. For example, assuming a number density of $n_{He'} \sim 0.08 \text{ cm}^{-3}$ [c.f. Eq.(4)] the mean distance between $He' - He'$ collisions is $1/(n_{He'} \sigma_{elastic}) \sim 0.03$ light years (using $\sigma_{elastic} \sim 3 \times 10^{-16} \text{ cm}^2$). One effect of the self interactions is to locally thermally equilibrate the mirror particles in the halo. The He' (and other mirror particles) should be well described by a Maxwellian velocity distribution with no cutoff velocity. [He' do not escape from the

⁴For detectors with more than one target element we must work out the event rate for each element separately and add them up to get the total event rate.

halo because of their self interactions]. A temperature, T , common to all the mirror particles in the halo can be defined, where $T = M_{A'} v_0^2/2$ (of course, T will depend on the spatial position). One effect of this is that v_0 should depend on $M_{A'}$ with $v_0(A') = v_0(He') \sqrt{M_{He'}/M_{A'}}$. Thus, knowledge of v_0 for He' will fix v_0 for the other elements. We will assume that the halo is dominated by He' (which is suggested by mirror BBN arguments[17]), with $v_0 \equiv v_0(He')$ in the range, Eq.(13).

The Earth motion around the sun produces an annual modulation in y :

$$y \simeq y_0 + \Delta y \cos \omega(t - t_0) \quad (14)$$

where $y_0 = \langle v_E \rangle / v_0$ and $\Delta y = \Delta v_E / v_0$ (for He' , $y_0 \approx 1.06$, $\Delta y \approx 0.07$). The parameter t_0 turns out to be June 2, and $\omega = 2\pi/T$ (with $T = 1$ year). Expanding $I(E_R)$ [Eq.11] into a Taylor series [making the y dependence explicit, i.e. $I(E_R, y) \equiv I(E_R)$]:

$$I(E_R, y_0 + \Delta y \cos \omega(t - t_0)) = I(E_R, y_0) + \Delta y \cos \omega(t - t_0) \left(\frac{\partial I}{\partial y} \right)_{y=y_0} \quad (15)$$

and

$$\left(\frac{\partial I}{\partial y} \right)_{y=y_0} = -\frac{I(E_R, y_0)}{y_0} + \frac{1}{\sqrt{\pi} v_0 y_0} \left[e^{-(x-y_0)^2} + e^{-(x+y_0)^2} \right]. \quad (16)$$

The net effect is an interaction rate

$$\frac{dR}{dE_R} = \frac{dR_0}{dE_R} + \frac{dR_1}{dE_R} \quad (17)$$

where

$$\begin{aligned} \frac{dR_0}{dE_R} &= \sum_{A'} \frac{N_T n_{A'} \lambda I(E_R, y_0)}{E_R^2} \\ \frac{dR_1}{dE_R} &= \sum_{A'} \frac{N_T n_{A'} \lambda \Delta y \cos \omega(t - t_0)}{E_R^2} \left(\frac{\partial I}{\partial y} \right)_{y=y_0}. \end{aligned} \quad (18)$$

Clearly, galactic mirror atom interactions will generate an annual modulation, $A \cos \omega(t - t_0)$, in the event rate coming from the $\frac{dR_1}{dE_R}$ component.

To compare these interaction rates with the experimental measurements, we must take into account the finite energy resolution and quenching factor. The quenching factor relates the detected energy (\tilde{E}_R) to the actual recoil energy (E_R),

$$\tilde{E}_R = q_{Na} E_R \quad (19)$$

and for the DAMA experiment, q_{Na} has been measured to be approximately $q_{Na} \simeq 0.30$ [1]. The energy resolution can be accommodated by convolving the rate with a Gaussian, with $\sigma_{res} \approx 0.16 \tilde{E}_R$ (from figure 3 of Ref.[29]).

The DAMA collaboration give their results in terms of the residual rate in the cumulative energy interval 2-6 keV, where they find that

$$A_{exp} = 0.020 \pm 0.003 \text{ cpd/kg/keV} \quad (20)$$

This number should be compared with the theoretical expectation:

$$A_{th} = \frac{1}{4} \sum_{j=0}^3 A_{th}^j \quad (21)$$

where

$$A_{th}^j \equiv \frac{1}{\Delta E} \int_{E_j}^{E_j + \Delta E} \int_0^\infty \frac{q_{Na} N_T n_{He'} \lambda \Delta y}{\tilde{E}'_R^2 \sqrt{2\pi} \sigma_{res}} \left(\frac{\partial I}{\partial y} \right)_{y=y_0} e^{\frac{-(\tilde{E}_R - \tilde{E}'_R)^2}{2\sigma_{res}^2}} d \tilde{E}'_R d \tilde{E}_R \quad . \quad (22)$$

with $E_j = 2.0 \text{ keV} + \Delta E * j$ ($j = 0, 1, 2, \dots$) and $\Delta E = 1.0 \text{ keV}$.

We have numerically studied A_{th} . We find that the O' contribution to DAMA/NaI dominates over the He' (H') contribution provided that $\xi_{O'} / \xi_{He'} \gtrsim 7 \times 10^{-4}$ ($\xi_{O'} / \xi_{H'} \gtrsim 4 \times 10^{-8}$). The reason for this is of course clear: the actual threshold recoil energy is 6.7 keV for $A' - Na$ interactions, which means that the v_{min} [from Eq.(5)] is:

$$\begin{aligned} v_{min}(H' - Na) &= 2830 \text{ km/s} \\ v_{min}(He' - Na) &= 795 \text{ km/s} \\ v_{min}(O' - Na) &= 290 \text{ km/s} \\ v_{min}(Fe' - Na) &= 166 \text{ km/s} \end{aligned} \quad (23)$$

Because $v_{min}(H' - Na) \gg v_0$, any H' contribution to the DAMA/NaI signal is expected to be very tiny and we will neglect it. The quantity $v_{min}(He' - Na)$ is also quite high which suppresses the He' contribution relative to O' and Fe' .

Interpreting the annual modulation signal in terms of He' , O' and Fe' , i.e. setting $A_{th} = A_{exp}$, we find numerically that:

$$|\epsilon| \sqrt{\frac{\xi_{He'}}{150} + \frac{\xi_{O'}}{0.10} + \frac{\xi_{Fe'}}{0.02}} \simeq 4.5 \times 10^{-9} \quad (24)$$

Because of the different masses of the three components, He' , O' , Fe' their relative contributions can potentially be determined by the differential recoil energy spectrum, A^j . In **Figure 1** we examine the representative possibilities a) DAMA signal is dominated by O' [i.e. $\xi_{O'} = 0.10$, $\xi_{A'} = 0$ for $A' \neq O'$], b) DAMA signal is dominated by Fe' [i.e. $\xi_{Fe'} = 0.02$, $\xi_{A'} = 0$ for $A' \neq Fe'$]⁵. The case where A_{th} is made up of approximately

⁵For interactions with Na , the form factor can be approximated to 1 because of the relatively low momentum transfer. Furthermore, it turns out that the $A' - Na$ interaction rate dominates over $A' - I$ interactions, except for the case of Fe' interactions in the 2 – 3 keV bin (A_{th}^0). For this bin (for Fe') there is significant uncertainty due to form factor uncertainties.

equal contributions from both O' and Fe' , corresponding to $\xi_{O'} = 5\xi_{Fe'} = 0.05$ is also given.

Implicit in our analysis is that the mirror atoms can reach the DAMA detector from all directions, without getting stopped in the Earth. The stopping distance of a mirror atom, A' (of energy $E' = \frac{1}{2}M_{A'}v^2$) in ordinary matter (of atomic number density $n = \rho/M_A$) can easily be evaluated from:

$$\begin{aligned}\frac{dE'}{dx} &= -\frac{\rho}{M_A} \int E_R \frac{d\sigma}{dE_R} dE_R \\ &= \frac{-\rho\pi M_{A'}\epsilon^2\alpha^2 Z^2 Z'^2 \ln\left(\frac{E_R^{max}}{E_R^{min}}\right)}{M_A^2 E'}\end{aligned}\quad (25)$$

where E_R^{max} can be obtained from Eq.(5) and $E_R^{min} = 1/(2r_0^2 M_A)$ (due to atomic screening). [Explicitly, $\ln\left(\frac{E_R^{max}}{E_R^{min}}\right) \approx 10$]. Eq.(25) can be solved to give the energy of the mirror atom after travelling a distance x through ordinary matter:

$$E'(x) = E'(0) \sqrt{1 - \frac{x}{L}} \quad (26)$$

where L is the stopping distance:

$$\begin{aligned}L &\simeq \frac{M_A^2 M_{A'} v_i^4}{8\pi\rho\epsilon^2\alpha^2 Z^2 Z'^2 10} \\ &\approx 10^5 \left(\frac{10^{-8}}{\epsilon}\right)^2 \left(\frac{v_i}{400 \text{ km/s}}\right)^4 \left(\frac{5 \text{ g/cm}^3}{\rho}\right) \left(\frac{2}{Z'}\right) \text{ km}\end{aligned}\quad (27)$$

where v_i is the initial velocity of the mirror atom. The stopping distance in earth for He' , O' and Fe' can easily be obtained from the above equation, giving:

$$\begin{aligned}L(He') &\gtrsim 10^7 \text{ km for } |\epsilon| = 4 \times 10^{-9}, v_i \geq v_{min}(He') \simeq 795 \text{ km/s}, \\ L(O') &\gtrsim 5 \times 10^4 \text{ km for } |\epsilon| = 4 \times 10^{-9}, v_i \geq v_{min}(O') \simeq 290 \text{ km/s}. \\ L(Fe') &\gtrsim 3 \times 10^3 \text{ km for } |\epsilon| = 4 \times 10^{-9}, v_i \gtrsim 200 \text{ km/s}.\end{aligned}\quad (28)$$

Since $L(He')$, $L(O')$ are much larger than the Earth's diameter, the retarding effect of the Earth is relatively small and no large diurnal effect is expected (in agreement with DAMA observations[30]). Mirror iron, may lead to a possibly large diurnal effect. However, dark matter detection experiments depend on $|\epsilon|\sqrt{\xi_{A'}}$ while the stopping distance in earth, depends just on $|\epsilon|$. The significant uncertainty in the size of $\xi_{A'}$ implies corresponding uncertainty in ϵ and hence $L(A')$. It is therefore still possible for the DAMA/NaI signal to be dominated by the Fe' component, without leading to any significant diurnal effect.

Let us now consider implications of this interpretation of the DAMA signal for other experiments. The CDMS/Ge experiment[25] has searched for nuclear recoils due to WIMP-Ge elastic scattering. This experiment has a threshold energy of 10 keV and

the quenching factor is *assumed* (but not measured!) to be 1. This experiment finds just 4 events satisfying their cuts with $10 \text{ keV} < E < 20 \text{ keV}$. However because the target consists of the relatively heavy element, Ge , and the threshold is relatively high, 10 keV, the sensitivity of the CDMS experiment to light mirror elements, is completely negligible. Assuming $|\epsilon| \sqrt{\xi_{O'}}/0.10 = 4.5 \times 10^{-9}$ (as suggested from the DAMA/NaI experiment, if O' dominates the rate), we find numerically that the number of O' induced events (above the 10 keV CDMS threshold) is much less than 1 for their exposure of 10.6 kg-day.

If there happens to be a significant Fe' component, then this may potentially be constrained by CDMS/Ge experiment. In the case where Fe' dominates the DAMA/NaI experiment, then $|\epsilon| \sqrt{\xi_{Fe'}/0.02} = 4.5 \times 10^{-9}$. Numerically, we find that this implies 16 events in the $10 \text{ keV} < E < 20 \text{ keV}$ range for CDMS, for their 10.6 kg-day exposure (c.f. just 4 detected events). However given possible experimental uncertainties, this case is not excluded. For example, the quenching factor may turn out to be slightly less than 1. For example, a value of 0.7 would reduce the expected number of events from 16 down to 5 events which is consistent with the data.

Clearly experiments with a lower threshold than DAMA/NaI might potentially provide more stringent constraints. The only experiment with a lower threshold than DAMA/NaI is the CRESST/Sapphire experiment[26]. That experiment uses 262 g sapphire crystals (Al_2O_3) as the target medium with a low detection threshold of $E_R(\text{threshold}) = 0.6 \text{ keV}$. These features make CRESST/Sapphire particularly sensitive to low mass dark matter particles such as He' , O' (and even Fe'). Unfortunately, the CRESST experiment does not have enough statistics to be sensitive to the annual modulation due to the Earth's motion around the sun, nevertheless the shape and normalization of the measured energy spectrum provide useful information. We now study in detail the implications of mirror matter-type dark matter for this experiment.

In this experiment the quenching factor is assumed to be approximately equal to 1 (however, again this has not been specifically measured)[26]. As with the DAMA/NaI experiment, the recoil spectrum, Eq.(9), needs be convolved with a Gaussian curve (with $\sigma_{res} \simeq 0.4247 \Delta E_{res}$ ⁶) in order to take into account the finite energy resolution of the detector,

$$\frac{d \tilde{R}}{d E_R} = \int_0^\infty \frac{dR(E'_R)}{d E'_R} \frac{1}{\sqrt{2\pi}\sigma_{res}} e^{\frac{-(E_R - E'_R)^2}{2\sigma_{res}^2}} d E'_R \quad (29)$$

The CRESST collaboration present their results in terms of the quantity,

$$C_j \equiv \frac{1}{\Delta E} \int_{E_j}^{E_j + \Delta E} \frac{d \tilde{R}}{d E_R} d E_R \quad (30)$$

⁶Note that $\sigma_{res} = \frac{\Delta E_{res}}{\sqrt{8 \ln 2}} \simeq 0.4247 \Delta E_{res}$ implies a FWHM of ΔE_{res} for the Gaussian curve, which is the CRESST prescription[26]. In Ref.[26], two values of ΔE_{res} are discussed, $\Delta E_{res} \approx 0.2 \text{ keV}$ (from an internal calibration source) and $\Delta E_{res} \approx 0.5 \text{ keV}$ (from possible contamination with ^{55}Fe). In our numerical work we have used the former value (unless otherwise stated). Using $\Delta E_{res} = 0.5 \text{ keV}$ would lead to $|\epsilon| \sqrt{\xi_{A'}}$ values smaller by about 20%.

where $E_j = 0.6 \text{ keV} + \Delta E * j$ ($j = 0, 1, 2, \dots$) and $\Delta E = 0.2 \text{ keV}$. We have numerically studied C_j for various cases. In **figure 2** we plot the expected value for C_j for the best fit values of $|\epsilon| \sqrt{\xi_{A'}}$ assuming the DAMA/NaI rate is dominated by a) O' , b) Fe' and c) 50-50 O' , Fe' mixture. [Recall, these are the same three cases which were fitted to the DAMA/NaI annual modulation signal and were plotted in figure 1]. As the figures show, the shape of the CRESST/Sapphire data (obtained from figure 10 of Ref.[26]) is reasonably consistent with the expected shape from A' interactions. This is due mainly to the fact that $d\sigma/dE_R \propto 1/E_R^2$ which happens to approximately coincide with the shape of the CRESST/Sapphire data. This is quite unlike the case of standard WIMPs which are predicted to have a much flatter distribution (see figure 10 of Ref.[26])⁷. Thus, it seems to be possible that the CRESST/Sapphire experiment may have detected A' interactions. Clearly, the normalization of the CRESST data favours the Fe' interpretation of the DAMA data, with the best fit about 20% high and O' is about a factor of 2 too high. The 20% normalization difference between the best fits of DAMA/NaI and CRESST/Sapphire is easily within expected systematic uncertainties. In **figure 3** we plot the CRESST best fit for Fe' , dark matter which corresponds to $|\epsilon| \sqrt{\xi_{Fe'}/0.02} = 4.0 \times 10^{-9}$. Also plotted is $|\epsilon| \sqrt{\xi_{Fe'}/0.02} = 4.5 \times 10^{-9}$ but with a CRESST quenching factor of 0.8 instead of the assumed value of 1.0. Figure 3 clearly demonstrates the rather nice fit of Fe' dark matter to the shape and normalization of the CRESST data (after allowing for reasonable systematic uncertainties).

Because of the systematic uncertainties it seems possible that the case of O' dominance of the DAMA/NaI data is still allowed. We illustrate this in **Figure 4**, where we assume a (CRESST) quenching factor of 0.7 (instead of the assumed value of 1.0), with $|\epsilon| \sqrt{\xi_{O'}/0.10} = 3.8 \times 10^{-9}$.

Given the rather nice fit of the shape and normalization of the CRESST data (within reasonable systematic uncertainties) to the expectations of Fe' , O' dark matter from the DAMA/NaI fit, it is clearly very tempting to suppose that the CRESST data may be mostly signal with very little background component. On the other hand, the CRESST collaboration[26] have argued that their data is most likely background because of the rate of coincidence events. This argument required the background to be isotropic which it may not be. Even if the coincidence events are isotropic, they may not necessarily be background. In particular, the presence of small mirror dust particles, which can be formed from oxygen and other elements (e.g. SiO_2) can have a large number of atoms (e.g. 10^{10}) which makes coincident events possible.

Finally, note that the CRESST/Sapphire experiment is much more sensitive to H' , He' than the DAMA/NaI experiment. Assuming a pure He' halo, i.e. $\xi_{A'} = 0$ for $A' \neq He'$, we find that the CRESST data suggest:

$$|\epsilon| \sqrt{\frac{\xi_{He'}}{0.5}} \approx 4 \times 10^{-9} \quad (31)$$

In this pure He' halo limit, the (CRESST) value for $|\epsilon| \sqrt{\xi_{He'}}$, above, is not consistent

⁷The reason for the different form of the cross section is that mirror matter interacts with ordinary matter electromagnetically via the exchange of massless virtual photons while in the standard WIMP case the interaction is point like.

with the value from DAMA/NaI [Eq.(24)]. Thus He' cannot dominate the rate for DAMA or CRESST. This suggests that: $\xi_{O'} \gtrsim 0.2\xi_{He'}$ and/or $\xi_{Fe'} \gtrsim 0.04\xi_{He'}$. Clearly this constraint is significant, but nevertheless, still allows He' to be the dominate halo dark matter component⁸.

Assuming that DAMA and CRESST have detected galactic mirror matter-type dark matter, then this suggests an $|\epsilon|$ value of around 10^{-8} – 10^{-9} . Previous work (see Ref.[13] and references there-in) looking at various solar system implications of mirror matter has identified a similar but somewhat larger range for ϵ , Eq.(3). This information is summarized in **figure 5**. Also shown is the experimental bound, $|\epsilon| \lesssim 10^{-6}$ coming from recent orthopositronium lifetime measurements[16] and also the limit suggested from BBN[31].

Let us also mention that if $|\epsilon| \sim 4 \times 10^{-9}$, there will be interesting terrestrial effects of mirror matter. Fragments (of size R) of impacting mirror matter space bodies can remain on/near the Earth's surface provided that[32]

$$R \lesssim 4 \left(\frac{|\epsilon|}{4 \times 10^{-9}} \right) \text{ cm.} \quad (32)$$

Such fragments can potentially be detected and extracted with a centrifuge[32]. If mirror matter fragments become completely embedded within ordinary matter (which is necessarily the case for $\epsilon < 0$) then the fragments will thermally equilibrate with the ordinary matter environment. The observational effect of this is to cool the surrounding ordinary matter, as heat is transferred to the mirror body and radiated away into mirror photons[33]. Finally, even tiny solar system mirror dust particles can lead to observable effects. These particles impact with the Earth with velocity in the range $11 \text{ km/s} \lesssim v \lesssim 70 \text{ km/s}$ and can produce bremsstrahlung photons as well as heat/vibrational energy, detectable in suitably designed surface experiments[34] such as the St. Petersburg experiment[35].

In conclusion, we have pointed out that the DAMA/NaI, CRESST/Sapphire and other dark matter experiments are sensitive to mirror matter-type dark matter. Furthermore, the annual modulation signal obtained by the DAMA/NaI experiment can be explained by mirror matter-type dark matter for $|\epsilon| \sim 4 \times 10^{-9}$. This explanation of the DAMA signal is supported by the size and shape of the CRESST data and is not in conflict with CDMS or any other dark matter experiment. This value of $|\epsilon|$ is also consistent with the value obtained from various solar system anomalies including the Pioneer spacecraft anomaly, anomalous meteorite events and lack of small craters on the asteroid Eros. It is also consistent with standard BBN.

Acknowledgements: The author would like to thank Profs. R. Bernabei, R. Cerulli, F. Probst for patiently helping me understand some details regarding their experiments.

⁸Note that the CRESST/Sapphire experiment does not put significant limits on the H' component of the dark matter halo. Numerically, we find that He' dominates over H' provided that $\xi_{H'} \lesssim 15\xi_{He'}$ which is not a very stringent condition.

The author also thanks R. Bernabei and R. Volkas for very valuable comments on a draft of this paper.

References

- [1] R. Bernabei et al. (DAMA Collaboration), *Phys. Lett.* B389, 757 (1996); *ibid* B424, 195 (1998); *ibid* B450, 448 (1999); *ibid* B480, 23 (2000); *Eur. Phys. J.* C23, 61 (2002); *Phys. Rev.* D61, 023512 (1999); *ibid* D66, 043503 (2002).
- [2] R. Bernabei et al. (DAMA Collaboration), *Riv. Nuovo Cimento.* 26, 1 (2003) [[astro-ph/0307403](#)].
- [3] R. Foot, [hep-ph/0207175](#); R. Foot, *Acta Phys. Pol.* B32, 2253 (2001) [[astro-ph/0102294](#)]; A. Yu. Ignatiev and R. R. Volkas, Talk given at the Australian Institute of Physics Congress, July 2002 [[hep-ph/0306120](#)]; Z. Silagadze, *Acta Phys. Pol.* B32, 99 (2001) [[hep-ph/0002255](#)]; R. Foot, *Shadowlands: Quest for mirror matter in the Universe*, Universal Publishers, FL, 2002.
- [4] R. Foot, H. Lew and R. R. Volkas, *Phys. Lett.* B272, 67 (1991).
- [5] R. Foot, H. Lew and R. R. Volkas, *Mod. Phys. Lett.* A7, 2567 (1992).
- [6] R. Foot, *Mod. Phys. Lett.* A9, 169 (1994) [[hep-ph/9402241](#)]; R. Foot and R. R. Volkas, *Phys. Rev.* D52, 6595 (1995) [[hep-ph/9505359](#)].
- [7] B. Holdom, *Phys. Lett.* B166, 196 (1986).
- [8] R. Foot, A. Yu. Ignatiev and R. R. Volkas, *Phys. Lett.* B503, 355 (2001) [[astro-ph/0011156](#)].
- [9] R. Foot and R. R. Volkas, *Phys. Lett.* B517, 13 (2001) [[hep-ph/0108051](#)].
- [10] J. D. Anderson et al., *Phys. Rev.* D65, 08004 (2002) [[gr-qc/0104064](#)].
- [11] R. Foot, *Acta Phys. Polon.* B32, 3133 (2001) [[hep-ph/0107132](#)]; R. Foot and T. L. Yoon, *Acta Phys. Polon.* 33, 1979 (2002) [[astro-ph/0203152](#)].
- [12] M. Morawska-Horawska, A. Manechi, *Przeglad Geofizyczny* 40, 335 (1995); J. A. Docobo, R. E. Spalding, Z. Ceplecha, F. Diaz-Fierros, V. Tamazian and Y. Onda, *Meteoritics & Planetary Science* 33, 57 (1998); A. Ol'khovatov, <http://olkhov.narod.ru/gr1997.htm>. The Jordan event, <http://www.jas.org.jo/mett.html>; N. V. Vasilyev, *Planet. Space Sci.* 46, 129 (1998) and references there-in; P. W. Haines, R. J. F. Jenkins and S. P. Kelley, *Geology*, 29, 899 (2001).
- [13] R. Foot and S. Mitra, *Astroparticle Phys.* 19, 739 (2003) [[astro-ph/0211067](#)].

- [14] A. F. Cheng et al., *Science* 292, 484 (2001).
- [15] S. L. Glashow, *Phys. Lett.* B167, 35 (1986); R. Foot and S. N. Gninenko, *Phys. Lett.* B480, 171 (2000) [hep-ph/0003278].
- [16] R. S. Vallery et al, *Phys. Rev. Lett.* 90, 203402 (2003).
- [17] Z. Berezhiani, D. Comelli and F. L. Villante, *Phys. Lett.* B503, 362 (2001) [hep-ph/0008105]; A. Yu. Ignatiev and R. R. Volkas, *Phys. Rev. D* (in press) [hep-ph/0304260]. For pioneering work, see also S. I. Blinnikov and M. Yu. Khlopov, *Sov. J. Nucl. Phys.* 36, 472 (1982); *Sov. Astron.* 27, 371 (1983).
- [18] D. N. Spergel et al. (WMAP Collaboration), *Ap. J.* (in press) [astro-ph/0302209].
- [19] R. Foot and R. R. Volkas, *Phys. Rev.* D68, 021304 (2003) [hep-ph/0304261].
- [20] C. Alcock et al. (MACHO Collaboration), *Astrophys. J.* 542, 281 (2000) [astro-ph/0001272].
- [21] Z. Silagadze, *Phys. Atom. Nucl.* 60, 272 (1997) [hep-ph/9503481]; S. Blinnikov, astro-ph/9801015; R. Foot, *Phys. Lett.* B452, 83 (1999) [astro-ph/9902065].
- [22] R. Foot, A. Yu. Ignatiev and R. R. Volkas, *Astropart. Phys.* 17, 195 (2002) [astro-ph/0010502].
- [23] R. Foot, *Phys. Lett.* B471, 191 (1999) [astro-ph/9908276]; *Phys. Lett.* B505, 1 (2001) [astro-ph/0101055].
- [24] See e.g. D. C. B. Whittet, *Dust in the galactic environment*, IOP, Bristol 1992.
- [25] R. Abusaidi et al. (CDMS Collaboration), *Phys. Rev. Lett.* 84, 5699 (2000).
- [26] G. Angloher et al. (CRESST Collaboration), *Astroparticle Phys.* 18, 43 (2002).
- [27] J. D. Lewin and P. F. Smith, *Astroparticle Phys.* 6, 87 (1996).
- [28] C. S. Kochanek, *Astrophys. J.* 457, 228 (1996).
- [29] R. Bernabei et al. (DAMA Collaboration), *Eur. Phys. J.* C18, 283 (2000).
- [30] R. Bernabei et al. (DAMA Collaboration), *Il Nuovo Cimento* A112, 1541 (1999).
- [31] E. Carlson and S. L. Glashow, *Phys. Lett.* B193, 168 (1987).
- [32] S. Mitra and R. Foot, *Phys. Lett.* B558, 9 (2003) [hep-ph/0301229].
- [33] R. Foot and S. Mitra, *Phys. Lett.* A315, 178 (2003) [cond-mat/0306561].
- [34] R. Foot and S. Mitra, hep-ph/0306228.
- [35] E. M. Drobyshevski et al., *Astronomical and Astrophysical Transactions*, Vol. 22, 19 (2003) [astro-ph/0108231]; astro-ph/0305597.

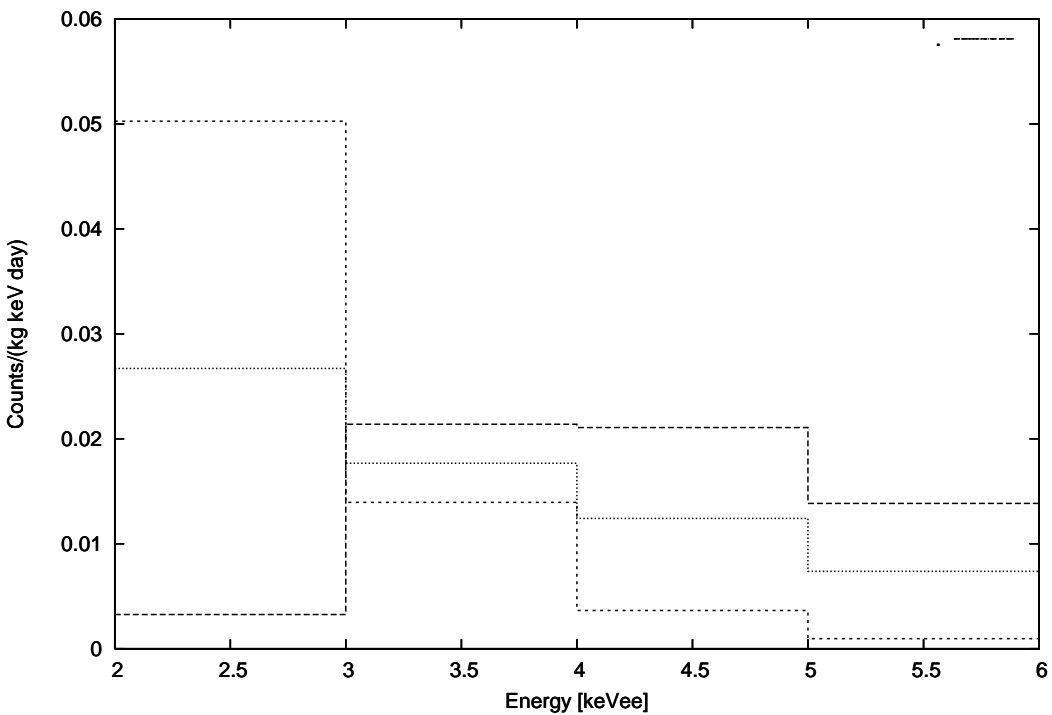


Figure 1: A_{th}^j (as defined in text) corresponding to the DAMA experiment for O' , Fe' dark matter (for $v_0 = 230$ km/s), with parameters a) $|\epsilon| \sqrt{\xi_{O'}/0.10} = 4.5 \times 10^{-9}$ (short-dashed line), b) $|\epsilon| \sqrt{\xi_{Fe'}/0.02} = 4.5 \times 10^{-9}$ (long-dashed line), c) $|\epsilon| = 4.5 \times 10^{-9}$ with $\xi_{O'} = 0.05, \xi_{Fe'} = 0.01$ (dotted line). In all three cases the differential rate in the 2-6 keV window agrees with the experimental value: $\sum_{j=0}^3 A_{th}^j \approx A_{exp}$ and the effect for $\tilde{E}_R > 6$ keV is negligible.

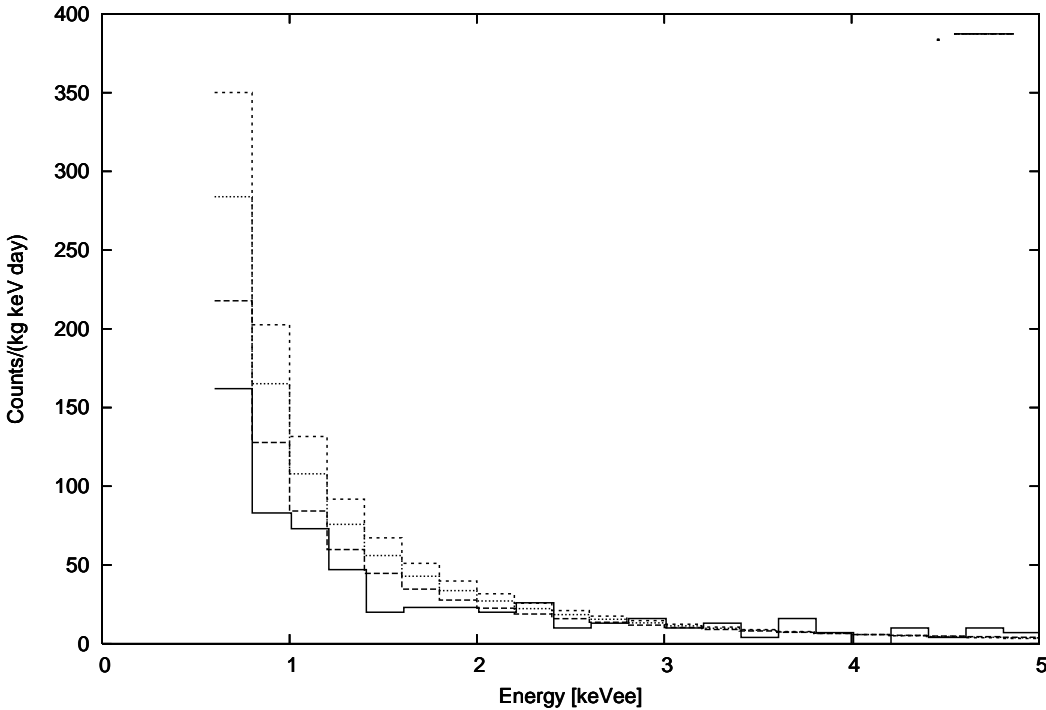


Figure 2: Expectation for the CRESST experiment for O' , Fe' dark matter with $v_0 = 230$ km/s and a) $|e|\sqrt{\xi_{O'}/0.10} = 4.5 \times 10^{-9}$ (short-dashed line), b) $|e|\sqrt{\xi_{Fe'}/0.02} = 4.5 \times 10^{-9}$ (long-dashed line), c) $|e| = 4.5 \times 10^{-9}$ with $\xi_{O'} = 0.05$, $\xi_{Fe'} = 0.01$ (dotted line). Also shown (solid line) is the CRESST data obtained from figure 10 of Ref.[26]. Note that the statistical errors in the data are $\sim 15 - 30\%$ for $E_R/\text{keV} = 0.6 - 2.0$ and $> 30\%$ for $E_R > 2.0$ keV.

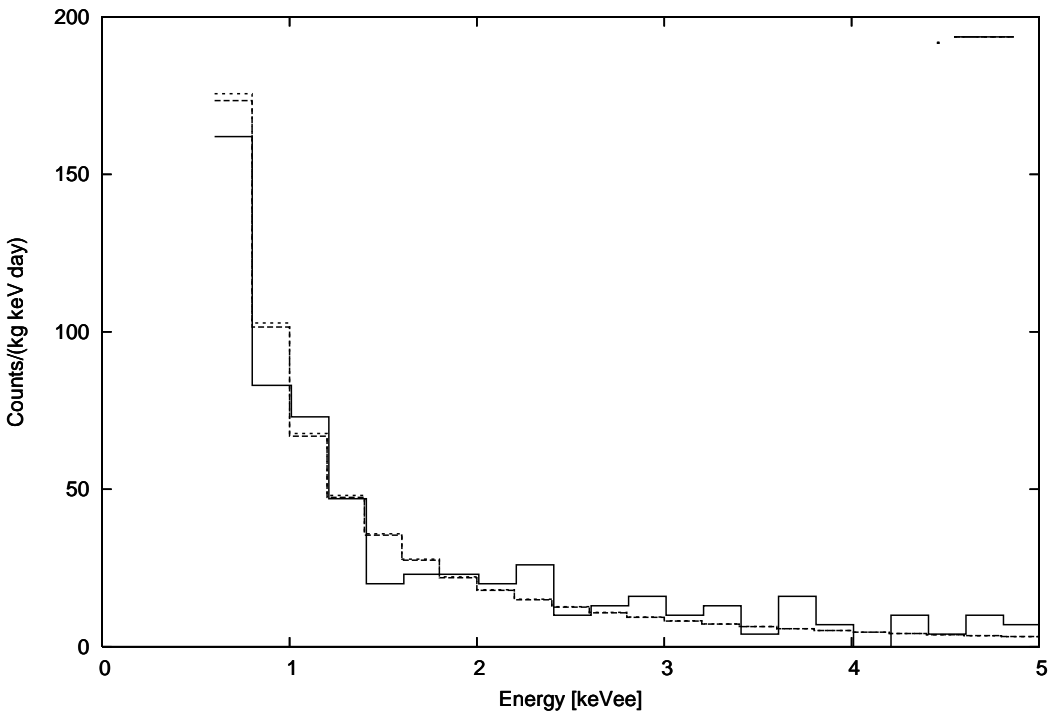


Figure 3: Expectation for the CRESST experiment for Fe' dark matter with $v_0 = 230$ km/s and a) $|\epsilon|\sqrt{\xi_{Fe'}/0.02} = 4.0 \times 10^{-9}$ (long-dashed-line), b) $|\epsilon|\sqrt{\xi_{Fe'}/0.02} = 4.5 \times 10^{-9}$ (short-dashed-line), with CRESST quenching factor of $q = 0.8$ (instead of 1). Also shown (solid line) is the CRESST data.

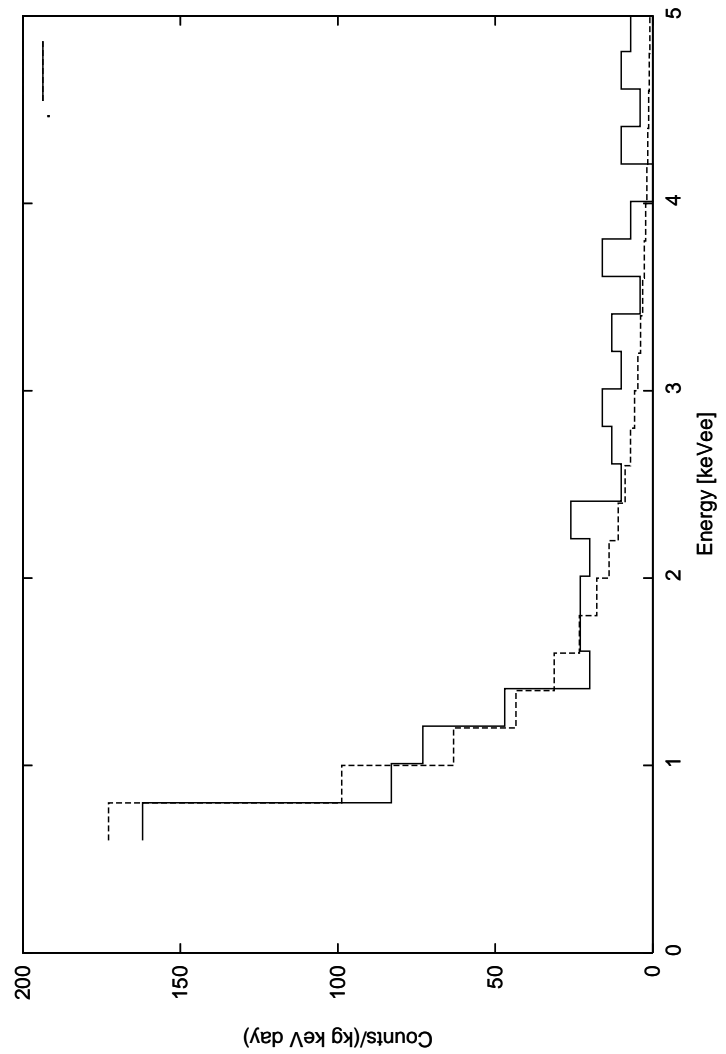


Figure 4: Expectation (dashed line) for the CRESST experiment for O' dark matter with parameters $v_0 = 230$ km/s and $|\epsilon| \sqrt{\xi_{O'}/0.10} = 3.8 \times 10^{-9}$, with CRESST quenching factor of $q = 0.7$ (instead of 1). The (solid line) is the CRESST data.

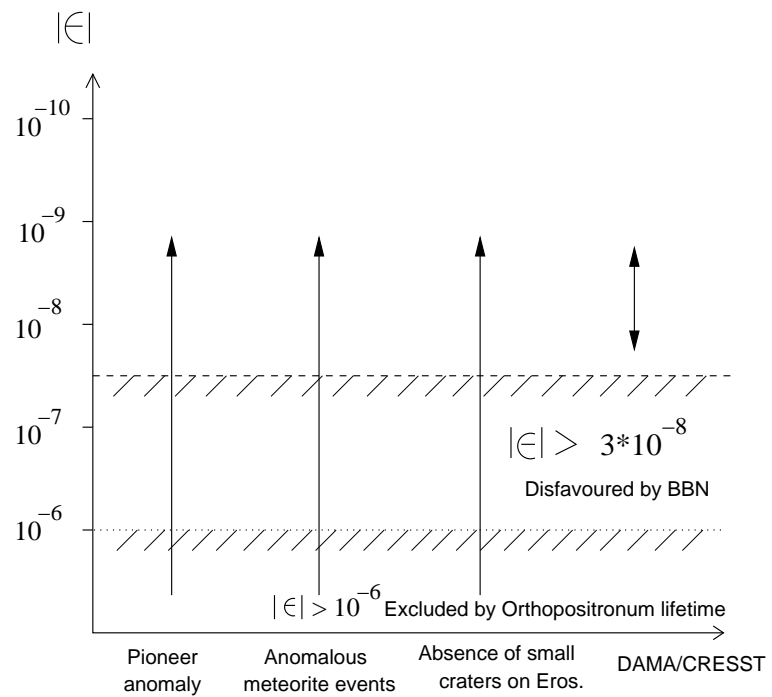


Figure 5: Favoured range of ϵ from various experiments/observations.